A Varactor-Tuned Helix-Based Chiral Layer

Farhad Bayatpur, Sara Wheeland, Alireza V. Amirkhizi, and Sia Nemat-Nasser

***Abstract*—Tuning performance of a chiral layer using varactor diodes is presented here. The chiral structure consists of an array of metallic long helices fabricated in parallel on a PCB. The helices have the same handedness, sub-wavelength diameter, pitch, and spacing in the array. Varactor diodes are incorporated into the array to tune array cross-polarized transmission response, a qualitative measure of the effective tuned chirality. Each helix is connected to one of its neighboring helices through a set of varactors placed between them. Array has one varactor per one helix pitch. The tuning performance of the chiral array transmissivity is measured over frequency band of 5.5–12 GHz with the bias voltage sweeping from 1 to 15 V. Voltage tuning changes each varactor capacitance from 0.9 to 0.13 pF. This results in $\sim$50% increase in the cross-polarization peak frequency, changing it from 6 to 9 GHz, for a linear polarization incidence perpendicular to the helices. Tuning rotates the transmitted wave polarization ellipse by $\sim 15^\circ$.**

***Index Terms*—Bianisotropic, chiral, polarization rotation, tunable.**

I. Introduction

CHIRALITY models the magnetic and electric fields' cross-coupling due to the material. This cross-coupling is usually reflected in the medium transmission response in form of a polarization rotation, [1], [2]. Chirality, as one of the material constitutive parameters, has direct influence on the medium refractive index. If strong enough, chirality could be designed to push the refractive index down to the vicinity of zero or perhaps negative values. This observation establishes the basis for designing engineered chiral materials with a negative index. In this approach, a negative refraction can be achieved without having simultaneously negative permittivity and permeability parameters [3]. This could simplify the design and fabrication.

Lakhtakia *et al.*, [4] introduced chiral nihility as a medium with a negative index. Having effective null permittivity and permeability parameters, this medium could support backward-wave propagation as a result of its significant chirality. Later, [5] claimed that a uniaxially chiral medium may actually support more eigenwaves with a negative index compared with isotropic chiral media and the left-handed materials. Experimental verification of nihility is an on-going research, [6]–[9].

Manuscript received January 22, 2013; accepted February 22, 2013. Date of publication April 11, 2013; date of current version May 06, 2013. This work was supported by the Air Force Office of Scientific Research (AFOSR) under Grant FA9550-09-1-0528 to the University of California, San Diego.

F. Bayatpur was with the Center of Excellence for Advanced Materials, Department of Mechanical and Aerospace Engineering, University of California, San Diego, La Jolla 92093 USA and is now with the Wireless Semiconductor Division, Avago Technologies, San Jose, CA 95131 USA.

S. Wheeland, A. V. Amirkhizi, and S. Nemat-Nasser are with the Center of Excellence for Advanced Materials, Department of Mechanical and Aerospace Engineering, University of California, San Diego, La Jolla 92093 USA (e-mail: sia@ucsd.edu).

Digital Object Identifier 10.1109/LMWC.2013.2253692

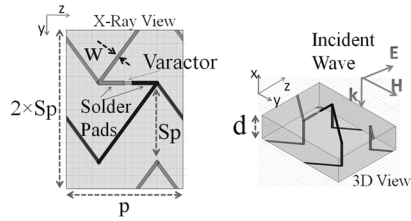

Fig. 1. Chiral array in one period with design parameters: 9 mm pitch (P); 6 mm spacing (Sp); 0.3 mm trace width (w); 2.2 dielectric constant of substrate; 3.2 mm substrate thickness (d); (C_v) 0.13–0.9 pF capacitance range.

As for the fabrication, maintaining all the requirements for a negative index state is a difficult task as designing a zero ϵ and a zero μ may be feasible only in a very narrow frequency band. In practice, the overall performance could be sensitive to the fabrication tolerances. In this scenario, a tunable design approach could be effective.

This letter explores the tunability of a non-resonant (wide band) chiral structure. Reversible mechanical tuning of an elastomeric polymer-helix composite was demonstrated in [10], where over 18% of chirality change was obtained by applying 30% axial strain. Taking an electronic approach, here, we aim at developing a helix-based tunable chiral structure. For tuning, varactors are incorporated into the design. Experiments test the performance and effectiveness of this tuning.

II. Design Specifications

Chiral composites often use asymmetrical and anisotropic building-blocks. Here, a chiral structure based on a metallic helix is considered. This structure consists of an array of 40×1 parallel long helices with varactor diodes mounted between them. Helices are all left-handed and are fabricated on a duroid PCB substrate. Each helix has 33 pitches.

A parallel helix array can be modeled as an effective chiral, uniaxial bianisotropic medium, [11], described using the tensorial form of the constitutive relations, $\bar{\mathrm{D}} = \bar{\bar{\epsilon}}\bar{\mathrm{E}} + \bar{\bar{\xi}}\bar{\mathrm{H}}$ and $\bar{\mathrm{B}} = \bar{\bar{\mu}}\bar{\mathrm{H}} + \bar{\bar{\zeta}}\bar{\mathrm{E}}$, [12]. For the helix array without the varactors, the constitutive parameters $\bar{\bar{\epsilon}}, \bar{\bar{\xi}}, \bar{\bar{\mu}}$ and $\bar{\bar{\zeta}}$ are all 3×3 complex-valued, diagonal matrices.

A. Unit Cell Geometry

Fig. 1 shows the chiral array arrangement in one period. The period (unit cell) consists of one pitch of two neighboring helices with a varactor placed between them. Loading the array by varactors this way can be shown that adds non-diagonal terms to the effective medium constitutive tensors. The unit cell dimensions are provided in Fig. 1 caption. With this unit cell, array requires 20×33 varactors. As shown, helices are in $\hat{z}$ with the incident wave normal to them in $\hat{x}$.

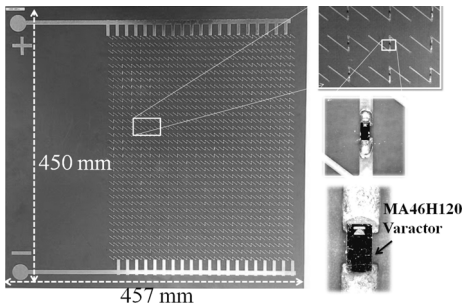

Fig. 2. Fabricated Sample top side loaded with MA46H120 varactor diodes.

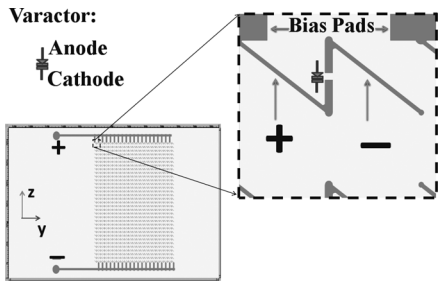

Fig. 3. Varactor (top) side of the helix array. Individual helices themselves are used as bias lines.

B. Fabrication

Fig. 2 shows the fabricated array (top side) loaded with MA46H120 varactors by M/Acom, Massachusetts, USA. Having a quality factor of better than 20 over 5–10 GHz, varactors add a few tenth of dB loss to the array total transmission.

Each varactor in the array connects a pair of neighboring helices. If connected to different voltages, these helices then can bias the varactors across them. This way, no additional traces are needed. Biasing scheme is demonstrated in Fig. 3. As shown, dc voltage is brought to the top side of the circuit by two thick horizontal lines. The bias line located above the array is biased at a higher voltage than the one below. Finally, consecutive helices in the array are attached to different bias lines to close the dc bias circuit. Using this scheme, varactors are all biased at once at the same voltage. Such biasing is insensitive to a single varactor failure and, therefore, is robust.

III. Experimental Results

The tunable sample is tested using a Transmit/Recieve setup, [13], in which the sample is placed half way between two lens-horn antennas with collimated beams. The following conventions assume that the sample varactor side is facing the antenna connected to port 2 of a Vector Network Analyzer.

Extracting the tunable array constitutive parameters including chirality requires a long discussion starting from a diagonal chirality case (see [14]). This is beyond the scope of this letter. Here, instead, we track the array polarization variation as a potential indication of chirality change.

Cross-polarization performance of the chiral array is measured under two incident polarizations upon the array top (varactor) side; 1) Axial $(\hat{z})$ incidence and 2) Perpendicular $(\hat{y})$ incidence. Fig. 4 shows the measured cross-polarized transmissions in case of axial $(S_{21}^{\parallel\perp})$ and perpendicular $(S_{21}^{\perp\parallel})$ incidents at different bias voltages from 1 to 15 V. This voltage sweep tunes the varactors' capacitance (C_v) from 0.9 to 0.13 pF. As shown, the

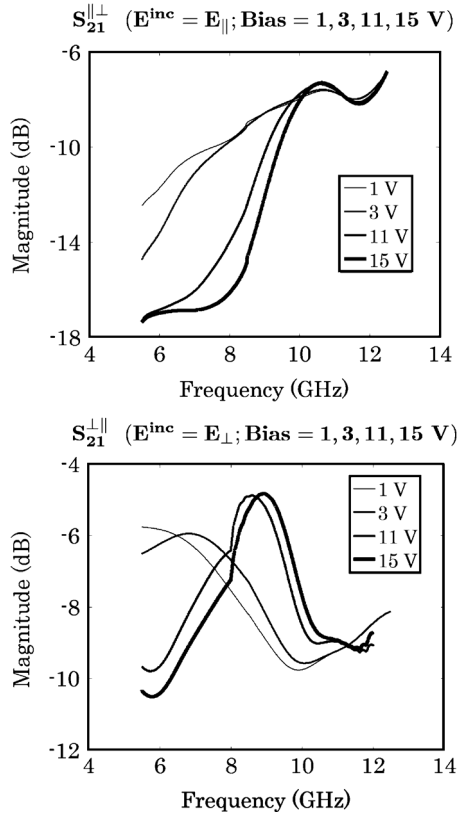

Fig. 4. (top) Axial incidence cross-polarization transmission, $S_{21}^{\parallel\perp}$; (bottom) Perpendicular incidence cross-polarization transmission, $S_{21}^{\perp\parallel}$.

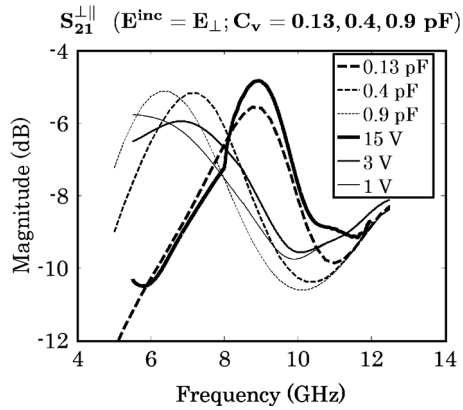

Fig. 5. $S_{21}^{\perp\parallel}$: measured (solid lines) against HFSS simulated (dashed lines).

decrease in $S_{21}^{\parallel\perp}$, while increasing the voltage, reaches a maximum of 5 dB at 8 GHz. This maximum for $S_{21}^{\perp\parallel}$ is observed at 9 GHz, which corresponds with a 5 dB increase in that cross-polarization.

HFSS simulations for a variable C_v are provided in Fig. 5, showing a good agreement with the measured data. Fig. 6 shows the tuned total transmission for axial and perpendicular incidences. Given the loss patterns observed in the transmissions and that a low-loss transparent layer is sought here, the proper band of operation for this chiral array falls between 9 and 10.5 GHz where the overall loss is minimal.

As expected, increasing the dc voltage decreases the capacitance, which in turn, shifts the frequency response to higher frequencies. Varactors create a cross path for current in addition to the array-alone (unloaded) current distribution along its

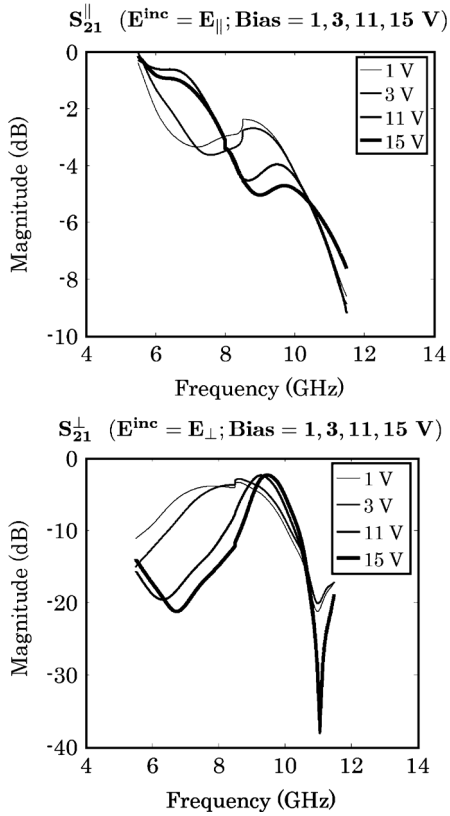

Fig. 6. (top) Axial incidence total transmission, $S_{21}^{\parallel}$; (bottom) Perpendicular incidence total transmission, $S_{21}^{\perp}$.

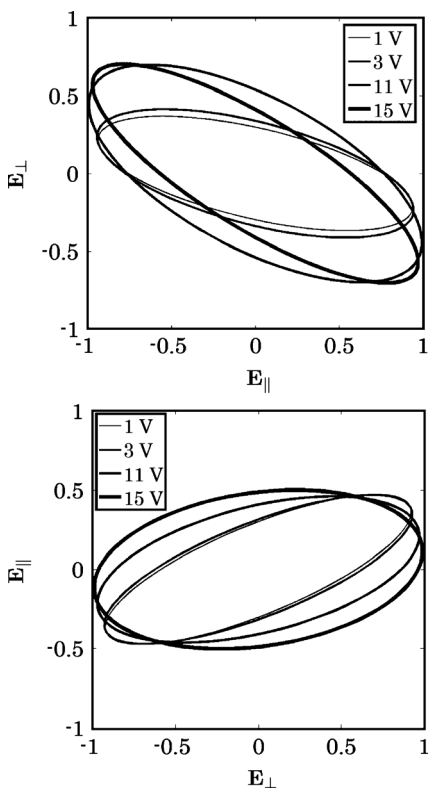

Fig. 7. (top) Transmitted wave polarization in axial incidence, $\mathrm{E}_{\perp}$ vs. $\mathrm{E}_{\parallel}$ and (bottom) in perpendicular incidence, $\mathrm{E}_{\parallel}$ vs. $\mathrm{E}_{\perp}$, both at 9 GHz.

helices. This current generates an additional scattering pattern that is superimposed to that of the unloaded array. Any variation in this current (for instance by capacitance tuning) changes the cross-polarization.

Capacitance change also alters the current distribution on the helical elements. This changes the self-inductance of the helices and their coupling. Inductance variations are expected to change the chirality, [10], which constitutes the second factor for cross-polarization tuning. Out of the two mechanisms described above, the second one seems to be dominant.

Polarization contours of the transmitted waves at 9 GHz for the two incidence conditions are provided in Fig. 7. As bias voltage increases, the polarization ellipses rotate clock-wise. Polarizations' rotation reaches a maximum of $\sim 15^{\circ}$ at 15 V for both incidences although it is slightly larger for the axial incidence (top plot in Fig. 7). While tuning, the polarization contours are slightly deformed.

IV. Conclusion

A tunable chiral composite consisting of an array of long, left-handed helices loaded with varactors is fabricated on a PCB. The helices themselves are used to bias all the varactors simultaneously. The array transmission response is measured for different bias voltages, from 1 to 15 V, corresponding to a capacitance tuning of 0.9 to 0.13 pF. The measured results exhibit a wide range of tuning in which the cross-polarization peak frequency is tuned from 6 to 9 GHz. This corresponds with 5 dB of variation in the cross-polarization levels at 6 and 9 GHz and $\sim 15^{\circ}$ of polarization rotation.

References

[1] W. S. Weiglhofer, A. Lakhtakia, and J. C. Monzon, "Maxwell-Garnett model for composites of electrically small uniaxial objects," *Microw. Opt. Tech. Lett.*, vol. 6, no. 12, pp. 681–684, Sep. 1993.

[2] M. M. I. Saadoun and N. Engheta, "A reciprocal phase shifter using novel pseudochiral or Ω medium," *Microw. Opt. Tech. Lett.*, vol. 5, pp. 184–188, 1992.

[3] D. R. Smith, W. J. Padilla, D. C. Vier, S. C. Nemat-Nasser, and S. Schultz, "Composite medium with simultaneously negative permeability and permittivity," *Phys. Rev. Lett.*, vol. 84, p. 4184, 2000.

[4] A. Lakhtakia, "An electromagnetic trinity from negative permittivity and negative permeability," *Int. J. Millim. Infrar. Waves*, vol. 22, pp. 1731–1734, 2001.

[5] Q. Cheng and T. J. Cui, "Negative refractions in uniaxially anisotropic chiral media," *Phys. Rev. B, Condens. Matter*, vol. 73, no. 113104, pp. 1–4, 2006.

[6] E. Plum, "Metamaterial with negative index due to chirality," *Phys. Rev. B, Condens. Matter*, vol. 79, no. 035407, pp. 1–6, 2009.

[7] S. Zhang, "Negative refractive index in chiral metamaterials," *Phys. Rev. Lett.*, vol. 102, no. 023901, pp. 1–4, 2009.

[8] R. Singh, "Terahertz metamaterial with asymmetric transmission," *Phys. Rev. B, Condens. Matter*, vol. 80, no. 153104, pp. 1–4, 2009.

[9] X. Xiong, "Construction of a chiral metamaterial with a U-shaped resonator assembly," *Phys. Rev. B, Condens. Matter*, vol. 81, no. 075119, pp. 1–6, 2010.

[10] S. Wheeland, F. Bayatpur, A. V. Amirkhizi, and S. Nemat-Nasser, "Elastomeric composites with tuned electromagnetic characteristics," *Smart Materials and Structures*, vol. 22, no. 1, p. 015006, Nov. 2012.

[11] I. V. Lindell, A. H. Sihvola, S. A. Tretyakov, and A. J. Vitanen, *Electromagnetic Waves in Chiral and Bi-Isotropic Media*. Norwood, MA: Artech House, 1994, ch. 8.

[12] J. A. Kong, *Electromagnetic Wave Theory*. Cambridge, MA: EMW Publishing, 2000, ch. 2.

[13] N. Gagnon, J. Shaker, P. Berini, L. Roy, and A. Petosa, "Material characterization using a quasi-optical measurement system," *IEEE Trans. Instrum. Measurement*, vol. 52, no. 2, pp. 333–336, Apr. 2003.

[14] F. Bayatpur, A. V. Amirkhizi, and S. Nemat-Nasser, "Experimental characterization of chiral uniaxial bianisotropic composites at microwave frequencies," *IEEE Trans. Microw. Theory Tech.*, vol. 60, no. 4, pp. 1126–1135, Apr. 2012.